Journal of Neuropathology and Experimental Neurology

Vol. 56, No. 4
April, 1997
pp. 440–454

Changes of NMDA Receptor Subunit (NR1, NR2B) and Glutamate Transporter (GLT1) mRNA Expression in Huntington's Disease—An In Situ Hybridization Study

THOMAS ARZBERGER, MD, KLAUS KRAMPFL, BSc, SUSANNE LEIMGRUBER, DMV, AND ADOLF WEINDL, MD, PhD

Abstract. The distribution of NMDA receptor subunit (NR1, NR2B) and glia-bound glutamate transporter (GLT1) mRNAs was investigated in postmortem brains of Huntington's disease (HD) patients and controls by means of in situ hybridization using radiolabeled deoxyoligonucleotides. In the neostriatum of HD, NR1, NR2B and GLT1mRNA decreased in correlation to disease severity. GLT1mRNA was not as low as NR1/NR2BmRNA. Losses were more prominent in putamen than in the distinctly atrophied caudate. NR1/NR2BmRNA decreased corresponding to neuronal loss, GLT1mRNA due to reduced cellular expression. The number of GLT1mRNA expressing cells identified as astrocytes increased in the neostriatum (astrogliosis). In contrast to controls, most of these astrocytes contained glial fibrillary acidic protein. NR1/NR2B and GLT1mRNA expression was not homogeneously lower in the neostriatum; zones with stronger hybridization signals corresponded to the matrix compartment and consisted of a larger number of cells with high mRNA levels. Early in the disease, cellular NR1/NR2BmRNA levels were higher in these zones than in controls. These findings indicate a loss of neurons with NMDA receptors in the neostriatum of HD. A concomitant proliferation of astrocytes with GLT1 transcripts may represent a compensatory mechanism protecting neostriatal neurons from glutamate excitotoxicity.

Key Words: Co-localization; Excitotoxicity; Glial fibrillary acidic protein; Glutamate transporter 1; Huntington's disease; In situ hybridization; NMDA receptor subunits.

INTRODUCTION

Huntington's disease (HD) is a completely penetrant autosomal dominant progressive neurodegenerative disorder caused by an expansion of CAG repeats (> 36) at chromosome 4p16.3 (1, 2). Huntington's disease manifests with choreatic hyperkinesia and cognitive and affective impairment, generally between 30 and 40 years of age (3). The most pronounced neuropathological change is atrophy of the neostriatum, the caudate being more severely affected than the putamen (4). This atrophy is characterized by an early loss of medium-sized spiny GABA/enkephalinergic neurons projecting to external pallidum, followed by losses of GABA/substance P-containing neurons projecting to substantia nigra pars reticulata and GABA/substance P-containing neurons projecting to the internal pallidum (5–8) and by a concomitant astrogliosis (9).

There are widespread glutamatergic projections from most cortical areas to the degenerating neostriatum (10, 11). Glutamate, the major excitatory neurotransmitter in the central nervous system of mammals, is a putative neurotoxin (excitotoxin) and is thought to be involved in neurodegeneration. It acts via ionotropic (AMPA, kainate, NMDA) or metabotropic receptors and is rapidly removed from the synaptic cleft by membrane-bound glutamate transporter proteins. Various pathophysiological mechanisms, including a defective glutamate transporter that might cause a prolonged stay or an increased concentration of glutamate in the synaptic cleft, an abnormally sensitive NMDA-receptor, or an abnormal number of NMDA-receptors, can lead to an increased influx of Na^+, Cl^- and Ca^{2+} ions with subsequent impairment of Ca^{2+} homeostasis, decrease in energy metabolism, and neuronal death (for review see reference 12).

NMDA receptors are composed of different subunits (NR1, NR2A, NR2B, NR2C, NR2D) (13). In human, 8 different splice variants of NR1 (NR1-1a/b, NR1-2a/b, NR1-3a/b, NR1-4a/b) (14), NR2A (15), NR2B (16) and 3 different glutamate transporters termed glutamate-aspartate transporter (GLAST), glutamate transporter 1 (GLT1), and excitatory amino acid carrier 1 (EAAC1), have been cloned so far (17–19). As found in rats, GLAST and GLT1 are mainly localized in membranes of glial cells, EAAC1 only in membranes of neurons (20, 21).

To investigate changes of the glutamatergic system in basal ganglia of HD, we examined brain tissue with short postmortem intervals of HD patients at different neuropathological stages of the disease and age-matched controls without any neurological disorder. Performing in situ hybridization using radiolabeled deoxyoligonucleotides, we focused on changes in the regional and cellular distribution of mRNA for NR1, which is essential for a functioning NMDA receptor (13), for NR2B, which is also expressed in basal ganglia, and for GLT1, the predominant glutamate transporter in mammalian brain (21, unpublished observations). The striosome-matrix compartmentation of the neostriatum was visualized by immunohistochemical staining of calbindin-D, a calcium-binding protein which is mainly localized in cell bodies

From the Department of Neurology, Technical University, Munich, Germany.

Correspondence to: Adolf Weindl, MD, PhD, Professor of Neurology, Neurologische Klinik der Technischen Universität München, Möhlstr. 28, 81675 München, Germany.

Supported by BMBF grant 9001KL.

TABLE 1
Patient Data

	#1	#2	#3
Sex	Male	Female	Male
Inheritance	Maternal	Paternal	Maternal
CAG repeats	45	48	44
Age at onset	40	23	32
Main symptoms	Onset with cognitive and affective impairment; later dementia; since age of 50, mild chorea	Onset with chorea; later cognitive and affective impairment	Onset with cognitive and affective impairment; later dementia and marked chorea
Age at death	60 years	40 years	64 years
Cause of death	cardiovascular failure	suffocation	cardiovascular failure
Neuropathological grade	2	3	4

and axons of neurons in the matrix (22) in relation to distribution patterns of NR1, NR2B and GLT1mRNA. In addition, glial fibrillary acidic protein (GFAP), an astroglia-specific type III intermediate filament protein (23, 24), was immunohistochemically stained in order to determine the extent of astrocyte proliferation in HD and to further characterize cells with GLT1 transcripts.

Patient Data and Methods

Preparation of Tissue: Brain specimens of 3 cases of HD (#1–3) with different neuropathological grades according to the classification of Vonsattel et al (25; clinical and pathological data are shown in Table 1) and of 3 age-matched controls (2 males and 1 female) without clinical evidence of neurological or psychiatric diseases were available from autopsies. The postmortem delay ranged from 8 to 14 hours (h). In all cases, a premortal agony could be excluded. Brains were cut into coronal slices of 1 cm thickness. Slices were immersion-fixed in 4% phosphate-buffered formaldehyde (pH 7.0) for 4 days and, for cryoprotection, transferred into 20% sucrose in phosphate-buffered saline (PBS; 0.1M PB, 0.15M NaCl, pH 7.2) until they sank to the bottom. Hemispheres were divided, cut into blocks with respect to anatomical structures, shock frozen with dry ice powder and stored at −80°C. Ten-μm serial sections were cut in a cryostat, thaw-mounted onto poly-l-lysine-coated slides, postfixed for 5 minutes (min) in 4% phosphate-buffered paraformaldehyde, and stored in 96% ethanol at 4°C until use.

In Situ Hybridization (ISH): Two different deoxyoligonucleotides (45 mers) complementary to coding parts of cDNAs specific for all splice variants of NR1 (oligo 1: 5′-CTC CTC CTC CTC CTC GCT GTT CAC CTT GAA CCG GCC GAA GGG GCT -3′, pos. 1570-1594 of splice variant NR1a; oligo 2: 5′-CGT GAC GGA GGT GGC ATT GAG CTG AAT CTT CCA GGA GCC GTG CCG -3′, pos. 154-178), NR2A (oligo 1: 5′-GCC GTT GAC CTC AAG GAC GAC CGA AGA TAG CTG TCA TTC ACC GCC -3′, pos. 4182-4226; oligo 2: 5′-GAC CAG AAG GGC CGG CAG CAC CAG CAG GGT CCA ATA GCC CAC TCT -3′, pos. 7-51), NR2B (oligo 1: 5′-GCT GAT GGA CCT GGA CTG GGT GGT GAA GGG TGG GTT GTC ACA GTC -3′, pos. 3013-3057; oligo 2: 5′-CCA TTG CTG GAG CCA TTG AAA GCC CTG GGG TTT TTG TTG TTA GGC -3′, pos. 4368-4412) or GLT1 (oligo 1: 5′-CTT CCT CAA CAC TGC AGT CGG CTG ACT TTC CAT TGG CTG CCA GAG -3′, pos. 1631-1675; oligo 2: 5′-GAG CCA AGA TGA CTG TCG TGC ATT CGC ACT TCC ACC TGC TTG GGC -3′, pos. 3-47) were synthesized (Pharmacia Biotech Benelux, Roosendaal, Netherlands).

ISH was performed under RNAase-free conditions according to the protocol of Wisden (26), with some modifications. Oligos were 3′-end labeled with α-^{33}P-dATP (Dupont, Bad Homburg, Germany) by terminal transferase (Boehringer Mannheim, Germany). A typical enzymatic reaction was performed for 30 min at 37°C, including 2 μl 5x tailing buffer (1M potassium cacodylate, 125 mM Tris-HCl, bovine serum albumin, 1.25 mg/ml, pH 6.6), 0.6 μl 25 mM $CoCl_2$, 1 μl 0.3 μM oligo1 or oligo2, 1 μl 5 mM α^{33}P-dATP, 25U terminal transferase, 5.5 μl sterile aqua dest and stopped with 40 μl 10 mM Tris/1 mM EDTA buffer, pH 8.0. Unincorporated nucleotides were removed by Bio-Spin 6 columns (Biorad, Munich, Germany). Only labels between 250,000 and 350,000 cpm per μl of the eluate were used for experiments. Sections were rehydrated in PBS, pretreated with 10 μg/ml proteinase K in 0.05M TRIS-HCl, 0.05M EDTA, pH 8.0 for 30 min at room temperature (rt), washed 3 × 5 min in PBS, transferred into 0.25% acetic anhydride in 0.1M triethanolamine-HCl pH 8.0/0.9% NaCl for 10 min, again dehydrated in ethanol and, finally, air-dried. Each section was hybridized for 20 h at 42°C with labeled probe diluted 1:50 in hybridization buffer containing 50% deionized formamide, 4 × standard saline citrate (SSC), 10% dextran sulfate, 100 μg/ml polyadenylic acid, 5 × Denhart's solution (bovine serum albumin, ficoll, polyvinylpyrrolidone each 1 mg/ml), 25 mM sodium phosphate (pH 7.0), 1 mM sodium pyrophosphate. After consecutive washes in 1 × SSC for 10 min at rt, 1 × SSC for 30 min at 55°C, 1 × SSC, 0.1 × SSC for 1 min each at rt and dehydration in ethanol, slides were air-dried. Neighboring sections were either exposed to βmax hyperfilm (Amersham, Braunschweig, Germany) for 20 days or dipped in Ilford K5 photoemulsion (Ilford, Dreieich, Germany) diluted 1:1 in sterile aqua dest and exposed for 28 days. In case of immunohistochemical co-localization, slides were transferred into PBS after dehydration. βmax hyperfilms were developed in Kodak D-19 for 5 min at 20°C and fixed in Kodak fixer for 15 min. Histoautoradiographs were developed for 3 min at 16°C and fixed for 2 × 3 min at rt. Dipped sections were counterstained with

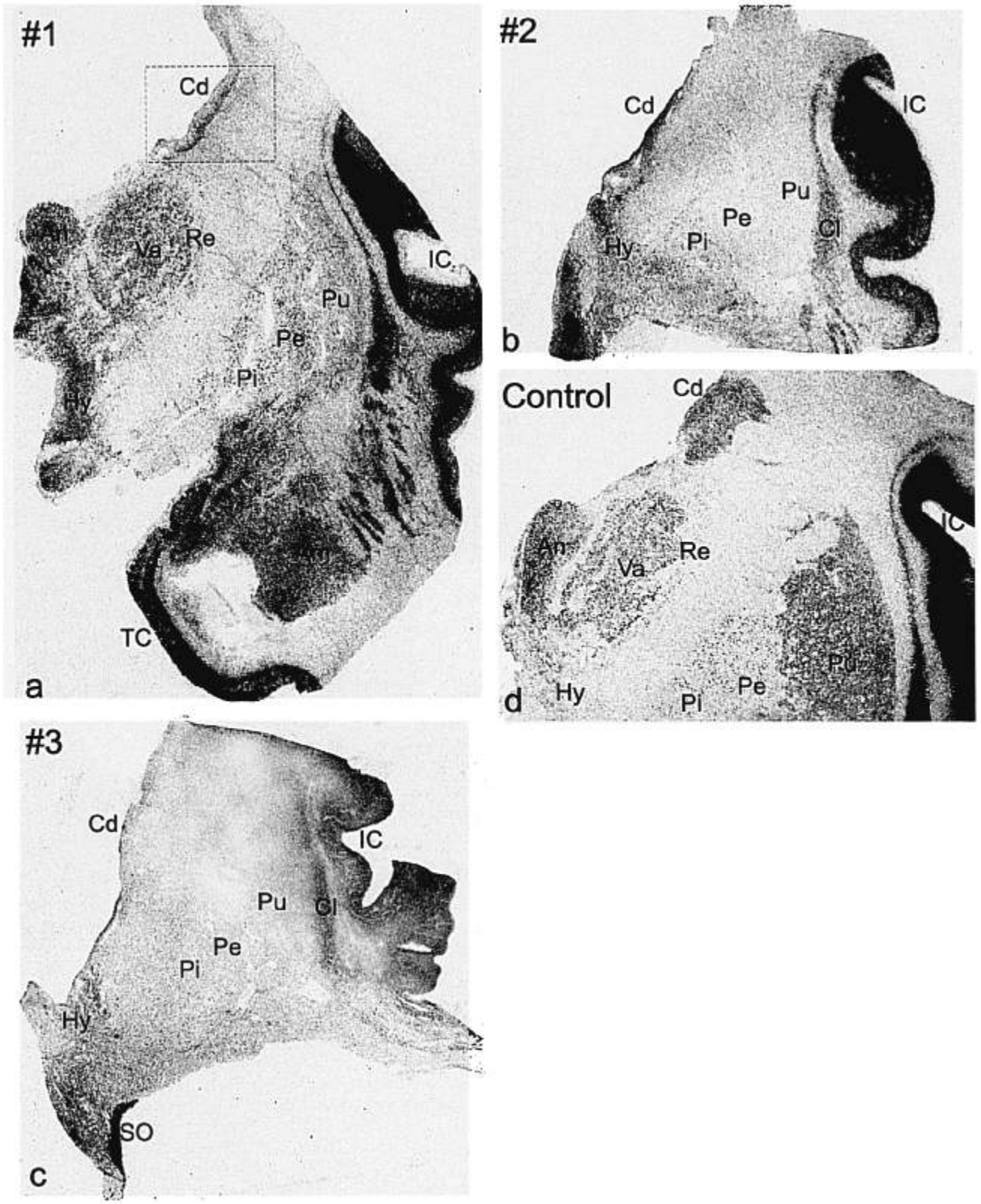

Fig. 1. NR1mRNA expression in 3 patients with increasing severity of HD (#1–3; a–c) and a control (d). Autoradiographs. βmax hyperfilms. Compared with the control, hybridization signals for NR1mRNA are reduced in the putamen (Pu) of #1 and are not detectable in the Pu of #2 or #3. In the distinctly atrophied caudates (Cd) of #1–3, NR1mRNA is still expressed, with more intense signals in the lateral caudate of #1 and medial caudates of #2 and #3. NR1mRNA expression does not appear to be affected in external (Pe) and internal pallidum (Pi) of #1 and Pi of #2, but is lower in Pe of #2 and is not detectable in Pi

0.5% toluidine blue, dehydrated in ethanol, cleared with xylene, mounted with Entellan (Merck, Darmstadt, Germany), and coverslipped.

Both oligos showed the same distribution pattern for each mRNA, confirming the specificity of our probes. Subsequently, all further experiments were performed using oligo 1 as the probe for each mRNA. For negative control, a 100-fold excess of nonlabeled oligonucleotides was added to the radioactive probe and applied to the adjacent section, leading to a complete suppression of the signal. Since no hybridization signals for NR2AmRNA were detectable in neostriatum of controls, experiments on HD tissue were omitted.

Immunohistochemistry (IHC)

GFAP and Calbindin-D Staining: Sections neighboring those where ISH had been performed were rehydrated in PBS. Endogenous peroxidase was blocked with 0.25% $KMnO_4$ for 5 min and washed in 1% oxalic acid/1% K_2SO_4 until $KMnO_4$ was completely washed out. Immunohistochemistry was performed according to the protocol given by DAKO (Hamburg, Germany). In brief, after preincubation with rabbit serum (1:10) in PBS, sections were incubated with a monoclonal mouse antibody directed against GFAP (Boehringer Mannheim, Germany), diluted 1:4, or against calbindin-D diluted 1:200 in PBS (Sigma, Deisenhofen, Germany), overnight at 4°C, followed the next day by an incubation with biotinylated rabbit-anti mouse IgG (1:300 in PBS) and a streptavidin-biotin-horseradish peroxidase complex (1:100 in 0.05M PB) for 30 min each at rt. The final enzymatic reaction was performed for 5 min using 0.01% H_2O_2 as substrate and 0.1% diaminobenzidine as chromogen in 0.05M PB. Counterstaining and mounting was the same as described for ISH. Unless otherwise stated, all chemicals for ISH and ICH were purchased from Sigma (Deisenhofen, Germany).

Co-localization of GLT1mRNA and GFAP: Combining ISH with IHC, IHC was carried out after ISH. Both techniques were performed as described above. After hybridization, washes in SSC and dehydration, slides were directly transferred into PBS for IHC. A pretreatment for blocking endogenous peroxidase was omitted. After the final enzymatic reaction, slides were dehydrated, air-dried, and dipped in photoemulsion.

Determination of Regional mRNA Levels: βmax hyperfilms were scanned with a Professional Desktop Scanner AGFA Arcus II (AGFA-Gevaert, Munich, Germany) at a resolution of 800 pixels per inch and a standardized grayscale ranging from 10 to 255.

Mean gray values were determined using the program NIH Image 1.52 for Macintosh (public domain). Images of coronal sections at the level of globus pallidus were evaluated. In order to receive absolute values comparable with measurements of different experiments, the mean gray value of each film was considered as background and subtracted. Anatomical areas of interest, such as caudate, putamen, external and internal pallidum, claustrum, insular cortex, and white matter were manually outlined with the cursor to compute their mean gray values. For each area, outlining and measuring were repeated 4 times and the mean value was noted. For each mRNA, images of neighboring sections of 4 different experiments were measured in the same way. The final mean gray value for each mRNA in each anatomical area of interest was calculated as the mean of the mean of all 4 experiments. In order to determine the correlation between gray values and intensity of radioactivity, each film was exposed to autoradiographic [^{14}C] micro-scale standards with a range from 0.1nCi/g to 100nCi/g (Amersham, Braunschweig, Germany) according to Akbarian et al (27). The mean gray value for each carbon-14 concentration was calculated the same way as described above for anatomical areas. With the help of the resulting calibration curve, each final mean gray value was converted into absolute values of radioactivity. Figure 4 shows all final mean values of radioactivity for NR1, NR2B and GLT1mRNA in selected anatomical areas of #1–3 and controls, after subtracting the mean values for white matter, which were considered to be nonspecific background; the values for controls represent the mean of the final mean values for all 3 controls.

Comparison of Cellular mRNA Levels: Only histoautoradiographs of the same experiment were selected for evaluation, in order to guarantee the same intensity of radioactivity, batch of photoemulsion, exposure time, and photochemical procedure. The number of silver grains per cell was compared between cells of similar size belonging to the same anatomical area of the same case or between corresponding cells of HD and controls.

RESULTS

1. Macroscopic Changes

All 3 cases of HD showed an atrophy of the neostriatum with a pronunciation of the caudate nucleus (Figs. 1a–c; 2a–c; 3a–c; 7a, b) in comparison with controls (Figs. 1d; 2d; 3d).

1a. Regional Distribution of NR1 and NR2BmRNA in Controls and HD Controls: At βmax hyperfilm level, NR1 and NR2B transcripts showed the same distribution pattern, with decreasing intensities in insular cortex, temporal cortex (not shown, n.s.), amygdala (n.s.), claustrum, supraoptic nucleus (n.s.), putamen, caudate, thalamus, external and internal pallidum, and hypothalamus (Figs. 1d; 2d; 4a, b). In comparison to NR2BmRNA, hybridization signals for NR1mRNA were stronger in external and internal pallidum, claustrum, insular cortex, and supraoptic nucleus, equal in the caudate, putamen, hypothalamus,

←

and Pe of #3. Signals in claustrum (Cl) and insular cortex (IC) are increasingly weaker from #1 to #3. There is no obvious reduction of expression in anterior (An), ventroanterior (Va) and reticular (Re) thalamic nuclei of #1 or hypothalamic areas (Hy) of #1–3 compared with the control. Strong signals remain in amygdala (Am) and temporal cortex (TC) of #1 and in supraoptic nucleus (SO) of #3. Inset represents detail enlarged in Figure 7a. a–d, ×2.

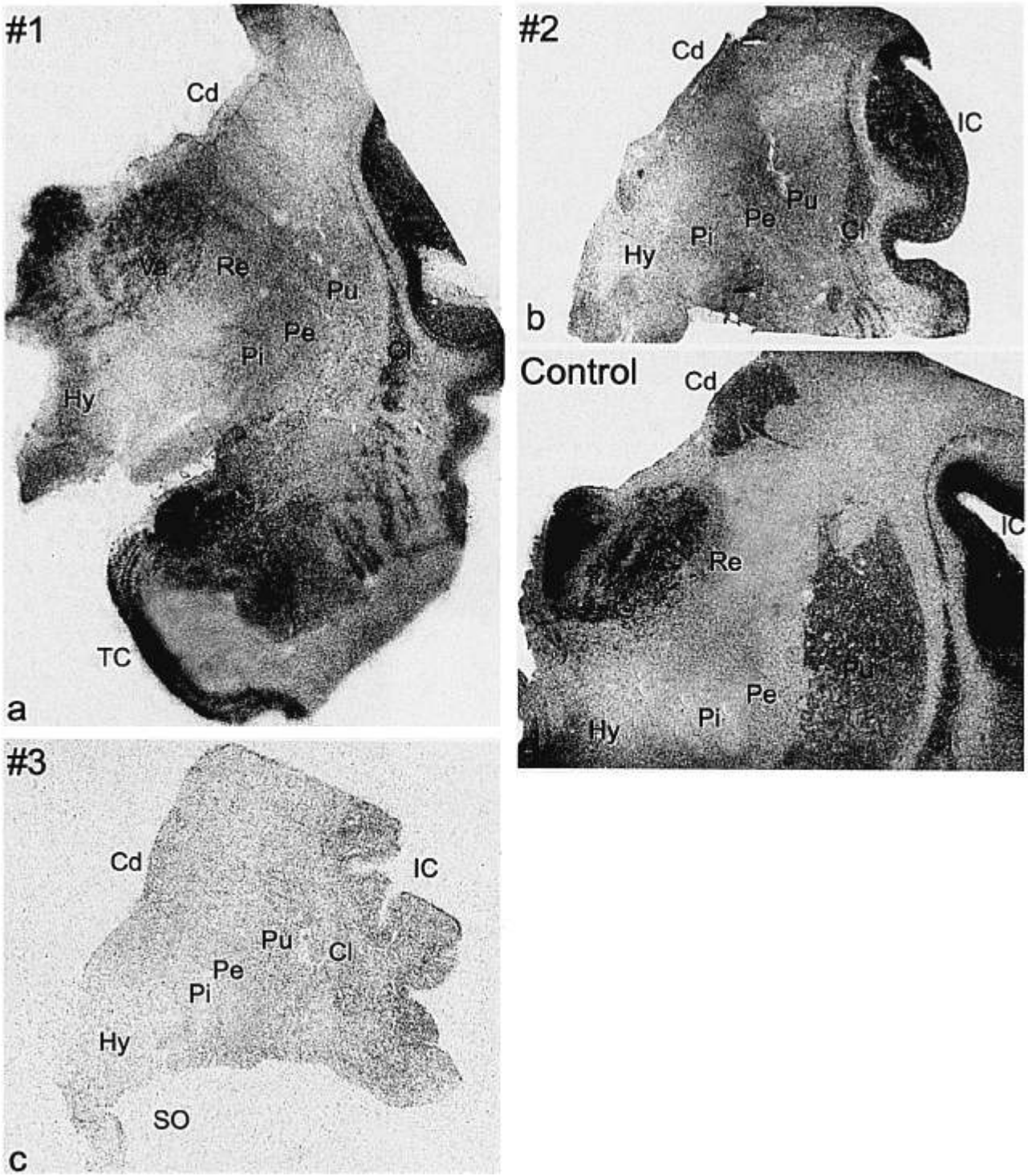

Fig. 2. NR2BmRNA expression in 3 patients with increasing severity of HD (#1–3; a–c) and a control (d). Autoradiographs. βmax hyperfilms. In sections adjacent to those of Figure 1, NR2B transcripts show the same distribution pattern as seen for NR1 transcripts (Fig. 1). Compared with NR1mRNA, hybridization signals for NR2BmRNA appear to be stronger in anterior (An), ventroanterior (Va), and reticular (Re) thalamic nuclei of #1 and the control, equal in caudate (Cd), putamen (Pu) of the control, amygdala (Am) and temporal cortex (TC) of #1, and weaker in all other areas in #1–3 and the control. Alterations of NR2BmRNA expression in #1–3 are the same as described for NR1mRNA (Fig. 1), except that there is no decrease in the external pallidum (Pe) of #2 and there is a reduction in An, Va, and Re of #1. Cl claustrum, Hy hypothalamus, IC insular cortex, Pe external pallidum, Pi internal pallidum, SO supraoptic nucleus. a–d, ×2.

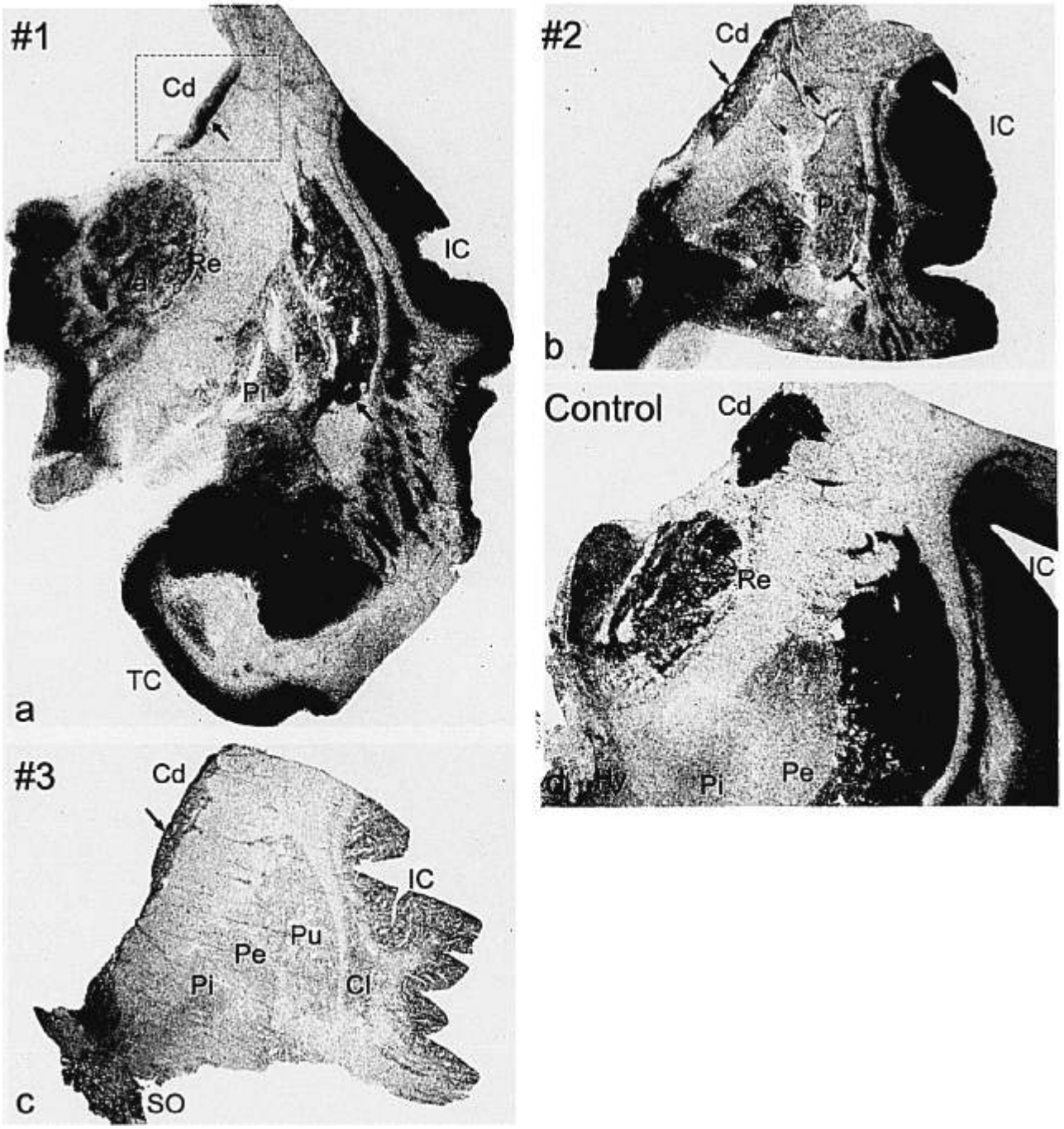

Fig. 3. GLT1mRNA expression in 3 patients with increasing severity of HD (#1–3, a–c) and a control (d). Autoradiographs. βmax hyperfilms. Sections adjacent to those of Figures 1 and 2. GLT1mRNA is present in the same areas that contain NR1/NR2B transcripts (Figs. 1, 2). In the atrophied putamen (Pu), GLT1mRNA expression is increasingly lower from #1 to #3. In the severely atrophied caudate (Cd) of #1–3, hybridization signals decrease to a similar degree. In both areas GLT1mRNA expression is not uniformly impaired. There are zones with more intense signals, including lateral caudate and ventral putamen of #1, medial caudate of #2 and #3, neostriatal cell bridges, and lateral and ventrolateral putamen of #2 (arrows). Compared with the control, there is a striking reduction of GLT1mRNA expression in the claustrum (Cl) and insular cortex (IC) of #3, a slight reduction in external (Pe) and internal pallidum (Pi) of #3, and no obvious reduction in Pe and Pi of #1, anterior (An), ventroanterior (Va) and reticular thalamic nuclei of #1 or hypothalamic areas (Hy) of #1–3. Signals in Pe and Pi of #2 appear to be stronger. Strong signals are seen in amygdala (Am) and temporal cortex (TC) of #1, and moderate signals are seen in supraoptic nucleus (SO) of #3. Inset represents detail enlarged in Figure 7b. a–d, ×2.

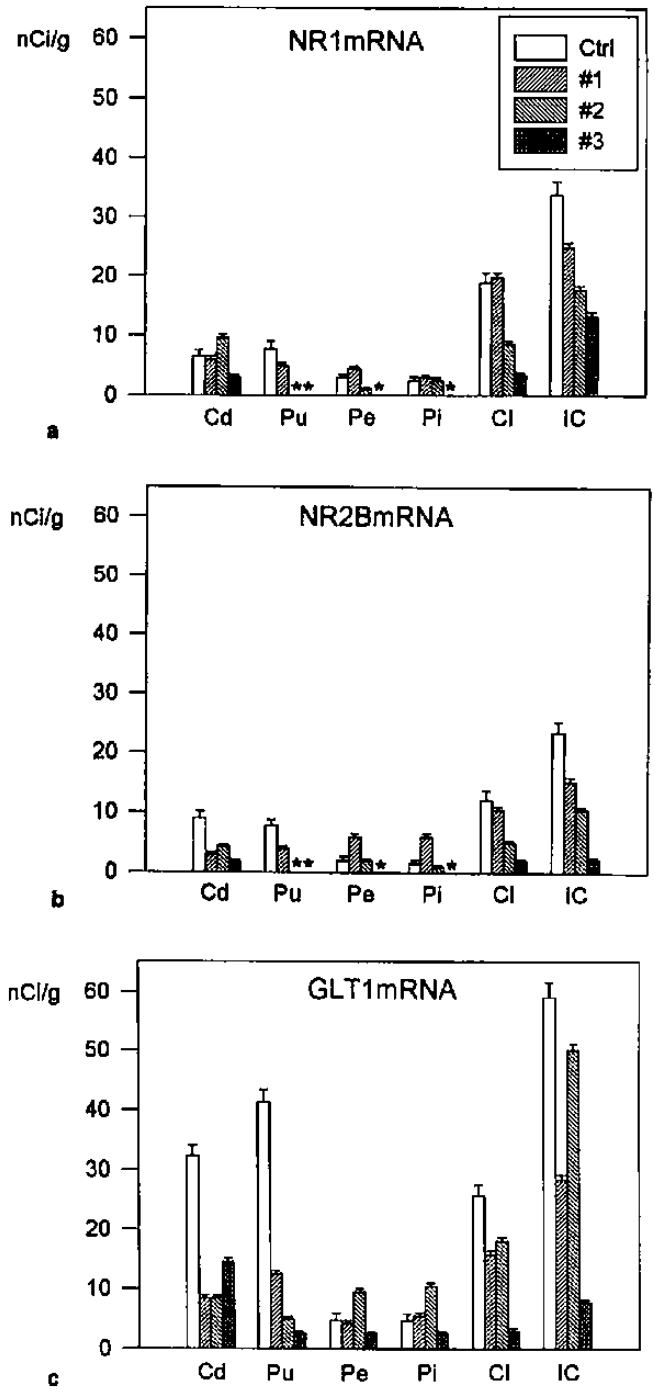

Fig. 4. Levels of NR1 (a), NR2B (b), and GLT1 (c) mRNA expression in caudate (Cd), putamen (Pu), external (Pe) and internal pallidum (Pi), claustrum (Cl), and insular cortex (IC) of #1–3 and controls. Data are shown as mean values ± SEM. Asterisks indicate values not discernible from zero counts.

amygdala (n.s.), and temporal cortex (n.s.), and lower in thalamus (Figs. 1d; 2d; 4a, b).

HD: Changes of mRNA expression were the same for NR1 and NR2B in all anatomical areas investigated with the exception of the external pallidum of #2 and the thalamus. In the neostriatum, both NR1 and NR2BmRNA expression was reduced compared with controls, with decreasing intensities from in #1 to #3 (Figs. 1a–d; 2a–d; 4a, b). The decrease was more prominent in the putamen than in the caudate. In the putamen of #1, moderate hybridization signals for NR1/NR2BmRNA were found (Figs. 1a; 2a; 4a, b), whereas in the putamen of #2 and #3, no signals were detectable at βmax level (Figs. 1b, c; 2b, c; 4a, b). In #1, signals in the dorsal part of the putamen were slightly lower than in the ventral part (Figs. 1a; 2a). In the caudate, the signals were not uniformly impaired—they were more intense in the lateral caudate of #1 (Figs. 1a; 2a; 7a) and medial caudate of #2 (Figs. 1b; 2b) and #3 (Figs. 1c; 2c). Compared with controls (Figs. 1d; 2d; 4a, b), the level of NR1/NR2BmRNA expression was not attenuated in the external and internal pallidum of #1 (Figs. 1a; 2a; 4a, b) and in the internal pallidum of #2 (Figs. 1b; 2b; 4a, b). In the external pallidum of #2, only NR1mRNA expression was lower (Figs. 1b; 2b; 4a, b). In the external and internal pallidum of #3, no hybridization signals for NR1/NR2BmRNA were detectable (Figs. 1c; 2c; 4a, b). In claustrum and insular cortex, NR1/NR2BmRNA expression was increasingly weaker from #1 to #3 (Figs. 1a–c; 2a–c; 4a, b) compared with controls (Figs. 1d; 2d; 4a, b). In the thalamus NR2B but not NR1mRNA expression was decreased. The reduction was more prominent in the ventroanterior than the anterior nucleus (Figs. 1a, d; 2a, d). No obvious reduction of NR1/NR2BmRNA expression was found in the hypothalamus (Figs. 1a–d; 2a–d), amygdala, temporal cortex (Figs. 1a; 2a; controls n.s.), or supraoptic nucleus (Figs. 1c; 2c; control n.s.).

1b. Regional Distribution of GLT1mRNA in Controls and HD Controls: GLT1mRNA was expressed in the same areas that contained NR1/NR2B transcripts. Hybridization signals for GLT1mRNA were intense in insular cortex, putamen, caudate, claustrum, amygdala (n.s.), thalamus, temporal cortex (n.s.), supraoptic nucleus (n.s.), and moderate in external and internal pallidum and hypothalamus (Figs. 3d; 4c).

HD: In the neostriatum of #1–3, GLT1mRNA expression was reduced compared with controls (Figs. 3a–d; 4c). Similar to NR1/NR2BmRNA, the decrease was more prominent in the putamen than in the caudate, but not to the same extent as seen for NR1/NR2BmRNA (Figs. 1; 2; 4). In the putamen, hybridization signals for GLT1mRNA were increasingly reduced from #1 to #3; in the caudate of #1–3, signals decreased to a similar intensity (Figs. 3a–c; 4c). In both areas, GLT1mRNA expression was not uniformly impaired. Zones with stronger hybridization signals were found in lateral caudate and ventral putamen of #1 (Figs. 3a; 7b), medial caudate, neostriatal cell bridges, lateral and ventrolateral putamen

of #2 (Fig. 3b), and medial caudate of #3 (Fig. 3c). Compared with controls (Figs. 3d; 4c), GLT1mRNA expression in external and internal pallidum was not altered in #1 (Figs. 3a; 4c), was enhanced in #2 (Figs. 3b; 4c), and was reduced in #3 (Figs. 3c; 4c). In the claustrum and insular cortex, signals decreased slightly in #1–2 (Figs. 3a, b; 4c), but distinctly in #3 (Figs. 3c; 4c) in comparison with controls (Figs. 3d; 4c). No obvious reduction of GLT1mRNA expression was found in hypothalamus (Fig. 3a–d), supraoptic nucleus (Fig. 3c; control n.s.), thalamus (Fig. 3a, d), amygdala and temporal cortex (Fig. 3a; control n.s.).

1c. Comparison of Zones with Prominent Hybridization Signals for NR1, NR2B or GLT1mRNA in the Neostriatum of #1–3 and Relation to the Striosome-matrix Compartmentation: In the caudate of #1–3 and the putamen of #1, zones with prominent hybridization signals for GLT1mRNA corresponded to zones with prominent hybridization signals for NR1/NR2B (Figs. 1a–c; 2a–c; 3a–c; 7a, b). However, in zones with prominent hybridization signals for GLT1mRNA in striatal cell bridges and putamen of #2 (Fig. 3b), no hybridization signals for NR1/NR2BmRNA were detectable at βmax level (Figs. 1b; 2b).

Immunohistochemical stainings of calbindin-D in neighboring sections revealed that zones with stronger hybridization signals for NR1/NR2B or GLT1mRNA corresponded to the remaining calbindin-D-rich matrix compartments (Fig. 5a, b).

Fig. 5. Comparison of GLT1mRNA hybridization signals (a) with the striosome-matrix compartmentation (b) in putamen of #2 on neighboring sections. a. Autoradiograph. βmax hyperfilm. b. Immunohistochemical staining of calbindin-D. In the putamen, zones with more intense hybridization signals for GLT1mRNA (a) correspond to dark-stained calbindin-D-rich matrix compartments (b; examples of corresponding areas are marked by arrows pointing to the same direction). Note the ventro-dorsal gradient of both hybridization signal intensity for GLT1mRNA and immunoreactivity for calbindin-D, indicating a dorso-ventral progression of degeneration in HD. ×7.

2. Microscopic Changes

2a. Cellular Changes in HD and GFAP Staining: In caudate and putamen of #1–3, there was a loss of neurons and an increase of GFAP-positive astrocytes (Fig. 6a) compared with controls (Fig. 6b). In external and internal pallidum, the increase of GFAP-positive astrocytes was less pronounced. In all these areas the somata of astrocytes had an oval shape and few short GFAP-positive processes (Fig. 6a), in contrast with somata of astrocytes of controls, which had a round shape and many long processes (Fig. 6b). No obvious changes concerning number and shape of GFAP-positive astrocytes were seen in hypothalamus, supraoptic nucleus, thalamus, amygdala, claustrum, and insular cortex of HD.

2b. Cellular Distribution of GLT1mRNA in Controls, Co-localization with GFAP, and Changes in HD

Controls: Cells with GLT1 transcripts were restricted to gray matter and equally distributed in all areas described above. Co-localization experiments for GLT1mRNA and GFAP revealed that all GFAP-positive astrocytes in gray matter contained GLT1mRNA, present not only in somata but also in processes (Fig. 6d), but the majority of cells with GLT1 transcripts were negative for GFAP. The distribution pattern of hybridization signals, present not only in somata, but also diffusely surrounding the somata (Figs. 7h; 8h), was the same in both GFAP-positive and GFAP-negative cells, suggesting that GFAP-negative cells were also astrocytes.

HD: In the caudate and putamen of all 3 cases of HD, the number of cells with hybridization signals for GLT1mRNA was higher (Figs. 6c; 7d, f; 8d, f) compared with controls (Figs. 7h; 8h). Rarely, a cell with GLT1 transcripts was found to be negative for GFAP. This was in contrast with caudate and putamen of controls and with all other areas investigated in controls and HD. Besides a slight increase of cells with GLT1 transcripts in external and internal pallidum, there were no obvious numerical alterations in other areas.

2c. Changes of Cellular GLT1mRNA Levels in HD: In the caudate and putamen of #1–3, cellular GLT1mRNA levels were constantly lower (Figs. 7d, f; 8b, d, f; 9b, d) than in corresponding areas of controls (Figs. 7h; 8h). Somata of neostriatal cells in controls were surrounded by a large halo of hybridization signals representing GLT1mRNA in cell processes (Figs. 7h; 8h). Corresponding to less extensively branching processes of astrocytes

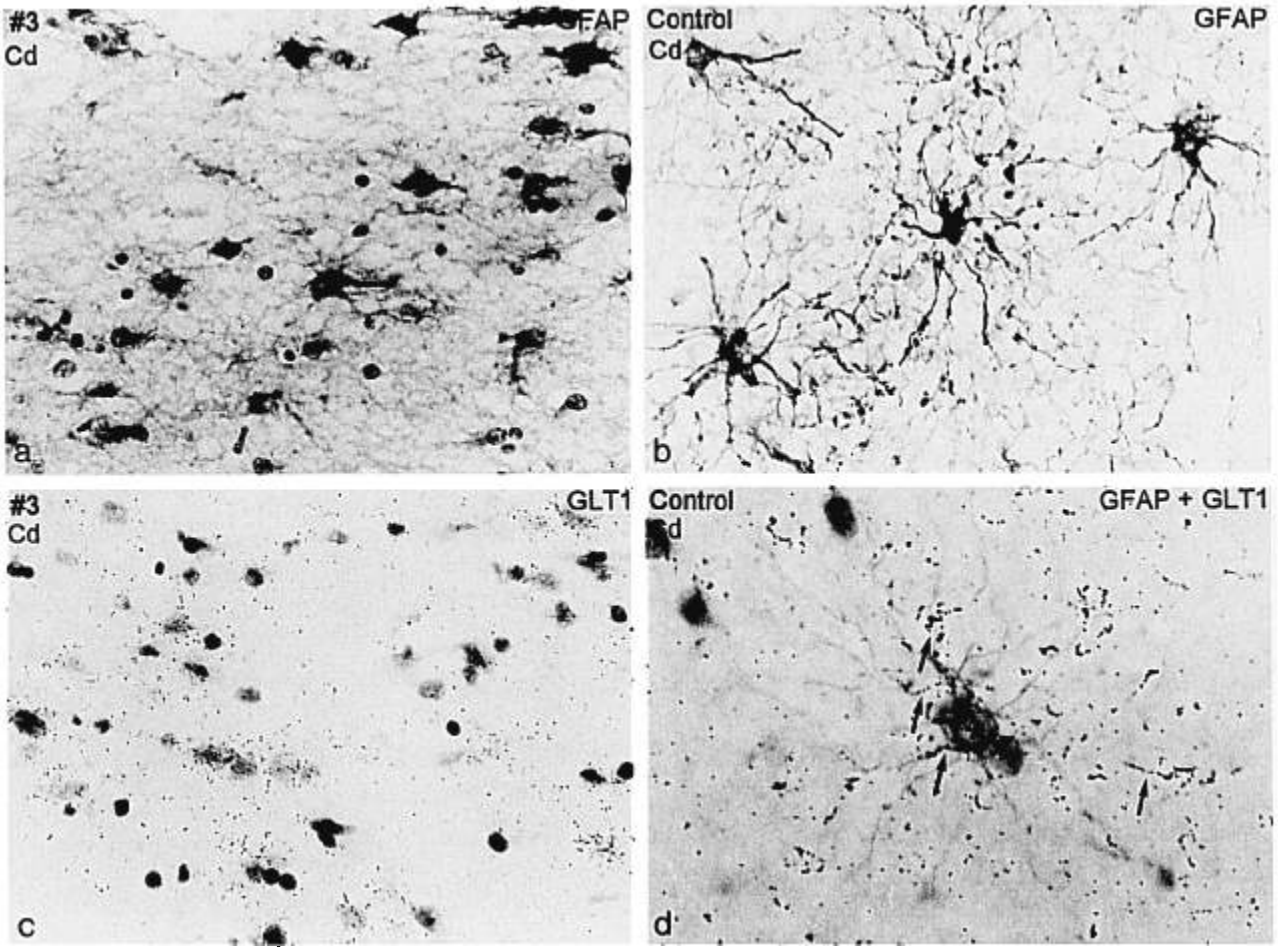

Fig. 6. Astrogliosis, GLT1mRNA expression in the caudate of #3 and characterization of a GLT1mRNA-containing cell. a, b, d. Immunohistochemical stainings for glial fibrillary acidic protein (GFAP). c, d. Histoautoradiographs for GLT1mRNA. In caudate (Cd) of #3 (a) the number of astrocytes, immunohistochemically marked for GFAP, is larger than in the control (b). Note the flat shape and less extensive branching processes of astrocytes in HD (a) compared with control (b). c. In Cd of #3, number and shape of cells with hybridization signals for GLT1mRNA (silver grains) are similar to GFAP-positive cells (a). d. A co-localization experiment reveals that GLT1mRNA is expressed in a GFAP-positive astrocyte in Cd of control. Hybridization signals are detectable in the soma as well as in processes (arrows). a–c, ×350. d, ×560.

in caudate and putamen of HD (Fig. 6a), the diameter of the halo of hybridization signals was smaller; GLT1 transcripts were mainly present in somata (Figs. 6c; 7d, f; 8b, d, f; 9b, d). In zones with prominent hybridization signals for GLT1mRNA at βmax level (Figs. 3a–c; 5a; 7b) corresponding to the remaining calbindin-D-rich matrix compartment (Fig. 5b), both the number of cells with GLT1 transcripts and their mRNA content were increased (Figs. 7f; 8b, d) compared with neighboring areas with less intense signals (Figs. 7d; 8f), which were calbindin-D poor. In other anatomical areas with reduced GLT1mRNA expression at βmax level, cellular mRNA levels were slightly lower in #1 and 2, and conspicuously lower in #3.

2d. Cellular Distribution of NR1- and NR2BmRNA in Controls and Changes in HD

Controls: In all areas investigated, the majority of cells with structural characteristics of neurons showed hybridization signals for NR1 and NR2BmRNA. In most types of neurons, NR2BmRNA levels were lower than NR1mRNA levels.

HD: In caudate and putamen, the number of cells with NR1 or NR2B transcripts was increasingly lower in #1–3. The loss was more prominent in putamen (Fig. 9c) than in caudate (Fig. 9a). No obvious numerical alterations were found in all other areas investigated.

2e. Changes of Cellular NR1/NR2BmRNA Levels in HD: In the caudate and putamen of #1, NR1/NR2BmRNA levels in most of the remaining neurons were similar or higher (Fig. 7c, e) than levels in corresponding neurons of controls (Fig. 7g); only in a few neurons were mRNA levels lower. This was in contrast to remaining neostriatal neurons of #2–3, in which NR1/NR2BmRNA levels were constantly lower (Figs. 8a, c, e; 9a) than in corresponding neurons of controls (Fig. 8g). In zones with prominent hybridization signals for NR1/NR2BmRNA at βmax level (Figs. 1a–c; 2a–c; 7a) corresponding to the remaining

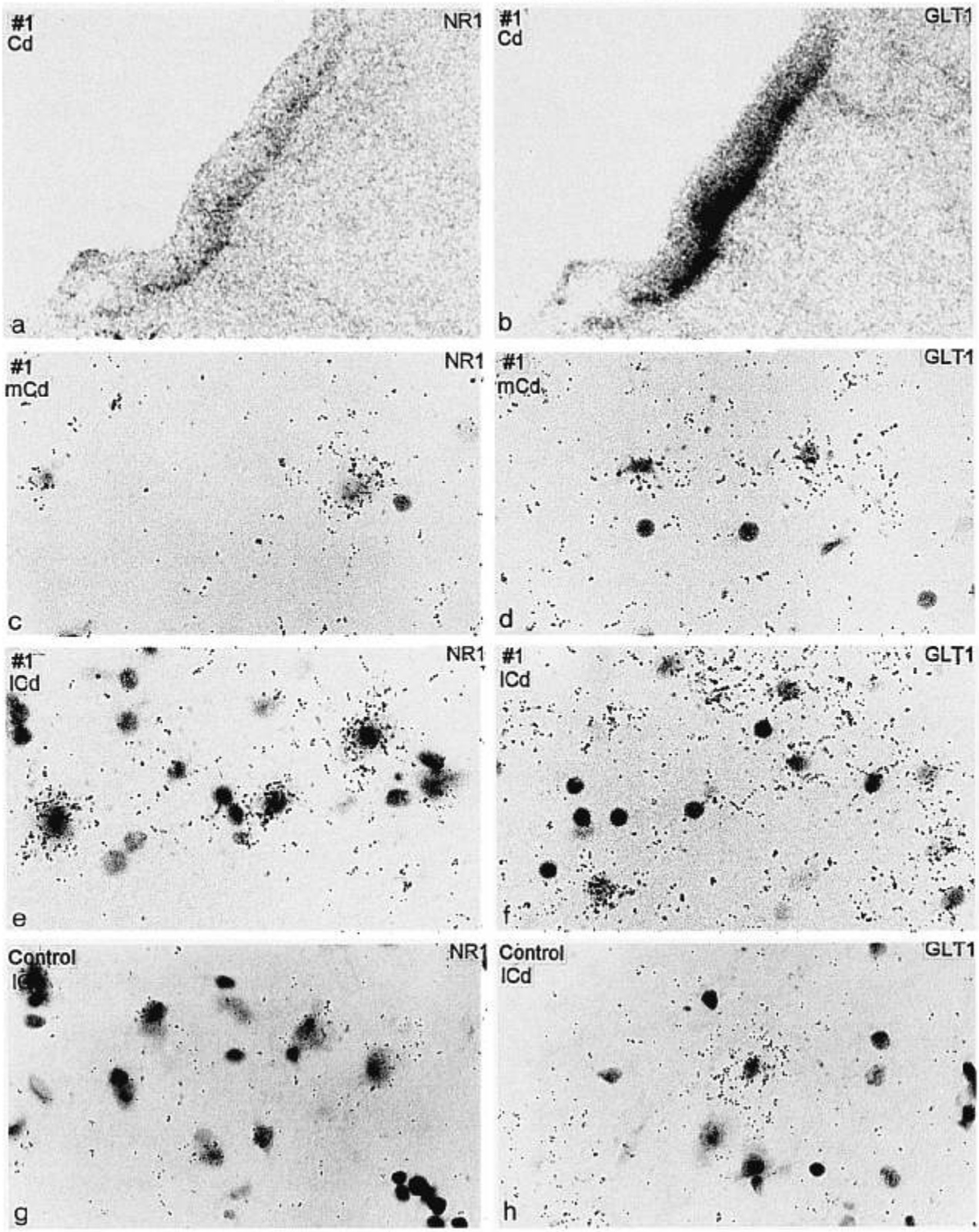

Fig. 7. NR1 (a, c, e, g) and GLT1mRNA (b, d, f, h) in caudate of #1 (a–f) and control (g, h). a, b. Survey. Details of Figures 1a and 3a. βmax hyperfilms. c–h. Histoautoradiographs. In #1, the expression of NR1 (a) and GLT1mRNA (b) is higher in lateral (lCd) than in medial caudate (mCd). The difference is more striking for GLT1mRNA. The number of cells with NR1 or GLT1 transcripts (silver grains) is enhanced in lCd (e, f) compared with mCd (c, d). The intensity of the hybridization signals for NR1mRNA is higher in neurons of lCd (e) than in neurons of mCd (c) or control (g). The number of cells containing GLT1mRNA is higher in lCd of #1 (f) compared with lCd of control (h). Note that the halo of silver grains surrounding the cell bodies and representing processes is larger in the control (h) than in HD (d, f). a, b, ×7. c–h, ×560.

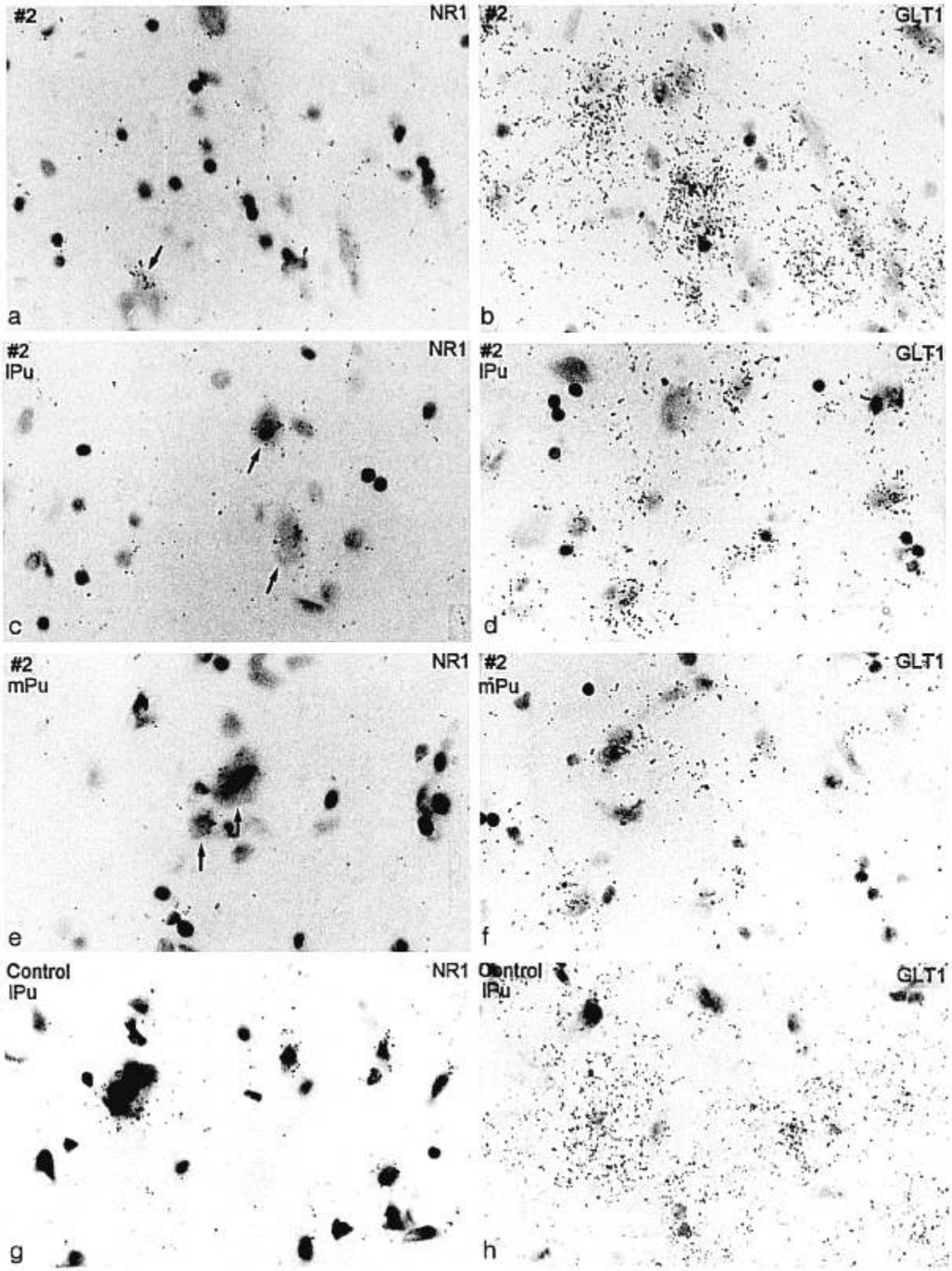

Fig. 8. Expression of NR1 and GLT1mRNA in neostriatal cell bridges (a, b) and putamen (c–f) of #2 (c–f) and control (g, h). Histoautoradiographs. In areas with pronounced hybridization signals for GLT1mRNA at βmax level, such as neostriatal cell bridges and lateral putamen (arrows in Fig. 3b), both the number of cells with GLT1 transcripts and the mRNA content is greater (b, d) compared with areas with less intense signals at the βmax level, such as the medial putamen (mPu; f and Fig. 3b). Comparing lateral putamen (lPu) of #2 (d) with lPu of control (h), the number of cells is larger in #2, but these cells do not

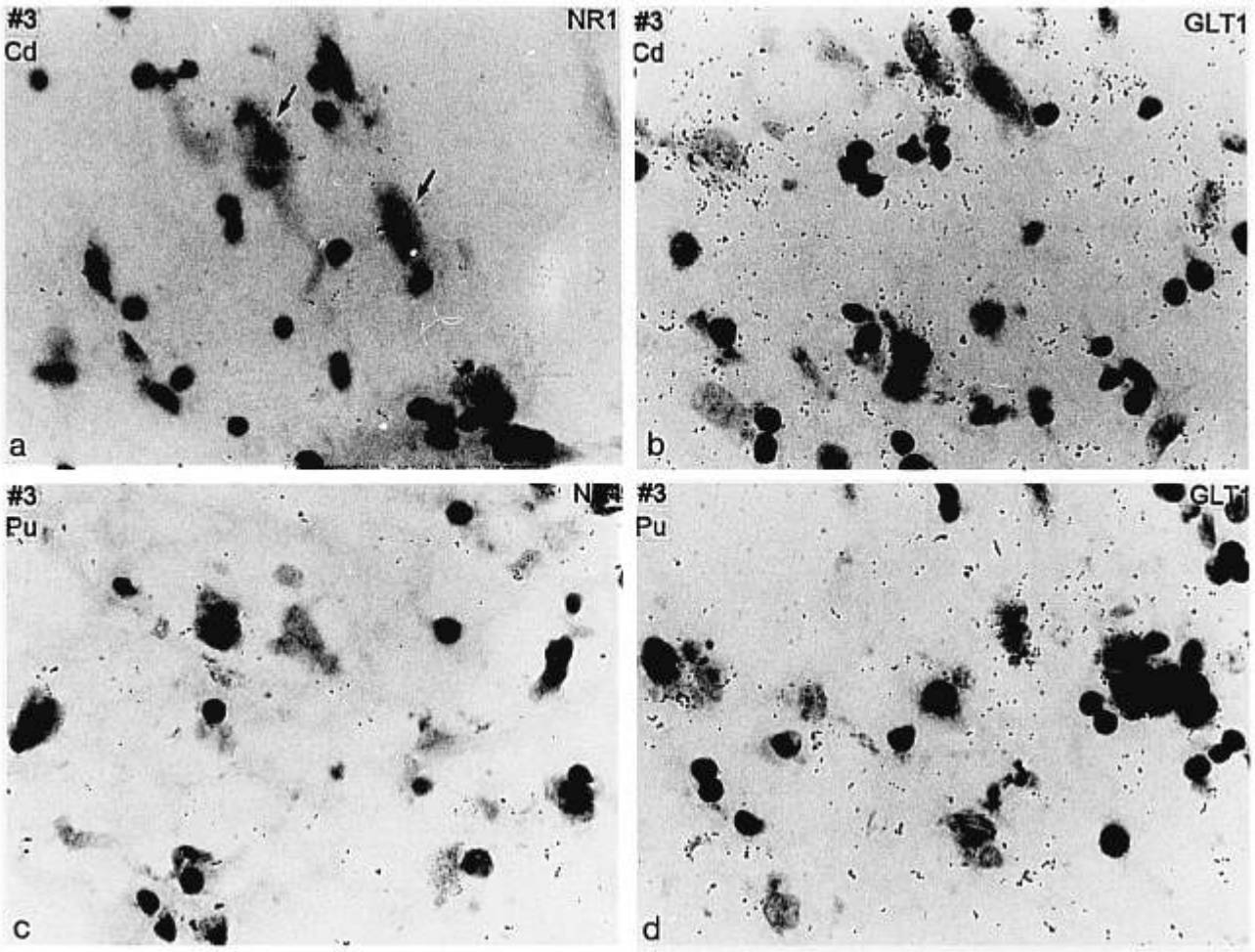

Fig. 9. NR1 and GLT1mRNA expression in the caudate (a, b) and putamen (c, d) of #3. Histoautoradiographs. a. In #3, the most severely affected case of HD investigated, only few neurons with low hybridization signals (silver grains) for NR1mRNA remain in the caudate (Cd, arrows). c. No signals are detectable in cells of the putamen (Pu; the few silver grains represent nonspecific background of photoemulsion). Both the number of cells with GLT1 transcripts and their mRNA content are higher in Cd (b) compared with Pu (d). a–d, ×560.

calbindin-D-rich matrix compartment, both the number of cells with NR1/NR2B transcripts and their mRNA content were higher (Fig. 7e) in comparison with neighboring areas with less intense signals (Fig. 7c); in #1, their mRNA levels were even higher (Fig. 7e) than in corresponding neurons of controls (Fig. 7g). In other areas of #1–3 with reduced NR1/NR2BmRNA expression at βmax level, cellular mRNA levels were lower.

DISCUSSION

In this study we investigated changes of the regional and cellular expression of NMDA receptor subunit (NR1/NR2B) and glutamate transporter (GLT1) mRNA in 3 cases of Huntington's disease of different levels of severity by means of in situ hybridization. The major findings were: (a) a gradual loss of NR1 and NR2BmRNA in neostriatum in correlation to the severity of the disease due to both a loss of neurons with NR1/NR2B transcripts and a decrease of mRNA expression in remaining neurons; the loss was more prominent in putamen than in the distinctly atrophied caudate. (b) Reduction of GLT1mRNA in neostriatum in correlation to the severity of the disease due to a decrease of cellular GLT1mRNA expression; the reduction was also more prominent in the

←

show the same extended halo of hybridization signals surrounding the cell bodies as seen in the control. This halo represents mRNA in astrocyte processes. In #2, only a few cells with very low hybridization signals for NR1mRNA (arrows) are present in neostriatal cell bridges (a), lPu (c) and mPu (e). In contrast with Cd of #1 (Fig. 7c, e), there is no difference in NR1mRNA content of cells belonging to zones with intense or weak hybridization signals for GLT1mRNA. As shown for lPu, cellular NR1mRNA levels are much higher in the control (g) than in HD (c). a–h, ×560.

putamen than in the caudate, but not as dramatic as seen for NR1/NR2BmRNA. (c) The reduction of NR1/NR2B and GLT1mRNA expression in neostriatum was not homogeneous. There was a ventro-dorsal gradient in the putamen of #1 and #2, a latero-medial gradient in the caudate of #1, but a medio-lateral gradient in #2 and #3. Zones with pronounced hybridization signals corresponded to the remaining matrix and consisted of a larger number of cells with enhanced mRNA levels. (d) The number of cells with GLT1 transcripts identified as astrocytes was higher in neostriatum (astrogliosis). (e) In contrast with controls, the vast majority of neostriatal astrocytes with GLT1 transcripts were GFAP-positive. (f) In the case with the lowest neuropathological grade (grade 2), cellular NR1/NR2BmRNA levels in zones with pronounced hybridization signals were higher than levels in corresponding neurons of controls.

HD is neuropathologically marked by a pronounced atrophy of the neostriatum, particularly of the caudate, due to a loss of neurons. With progression of the disease, neuronal loss in various other subcortical and cortical areas becomes apparent (28). Our observations of a marked loss of NR1 and NR2BmRNA in neostriatum and a reduction in pallidum, claustrum and insular cortex in HD indicate that NR1 and NR2BmRNA expressing neurons are severely affected. The loss of hybridization signals for NR1/NR2BmRNA in neostriatum is in accordance with earlier reports on decreased ligand binding to NMDA receptors (29, 30). It is speculated that the elongated polyglutamine stretch in the protein termed "huntingtin," which is coded by the increased number of CAG repeats in the "interesting transcript" (IT) 15 gene on chromosome 4 in HD, is involved in a potentiation of NMDA-receptor activation (2). Williams (25) reported that polyamines binding to recombinant NMDA-receptors, especially to heteromeric NR1a/NR2B receptors, in cell culture can lead to a long-term Ca^{2+}-influx, causing neuronal death. Thus, glutamate could act as an excitotoxin on neurons with modified, abnormally sensitive, NMDA receptors. Illarioshkin et al (32) and Furtado et al (33) found that a greater number of CAG repeats results in an earlier age at onset, a faster progression of neurological and psychiatric symptoms and a greater neuronal loss in neostriatum. The case with the longest CAG repeat length, #2, showed the earliest age at onset and the fastest clinical progression, in accordance with these observations. However, there was no positive correlation between CAG repeat length and neuropathological severity in our limited number of cases. Case #2 did not show the most pronounced neuropathological changes, possibly due to the fact that this patient died accidentally at a relatively young age. Cases #1 and #3, both having similar CAG repeat length, differed in neuropathological grading.

As we demonstrated, astrocytes express mRNA for the membrane-bound glutamate transporter GLT1, which is responsible for a rapid removal of glutamate from the synaptic cleft. Thus, the proliferation of astrocytes containing GLT1 transcripts found in HD might lead to an increased number of transporter proteins. The astrogliosis occurs in parallel with a progressive loss of neurons and is already present at neuropathological grades 0 and 1 (20, 34). Hedreen and Folstein (34) described a moderate-to-marked degree of astrocytosis in striosomes and a mild-to-moderate degree of astrocytosis in matrix at neuropathological grade 0, but a notable decrease of neuronal density only in striosomes, indicating that a proliferation of astrocytes occurs before neuronal degeneration. Therefore, the increase of astrocytes containing glutamate transporter mRNA could represent a compensatory mechanism to protect neurons from the excitotoxic effect of glutamate. With progression of the disease and loss of neurons with NMDA receptor transcripts, the expression of GLT1mRNA in astrocytes appears to be downregulated, as our observations indicate. This is in accordance with observations of Cross et al (35), who found a reduction of high-affinity glutamate uptake sites in postmortem neostriatum of HD. The downregulation may be due to a loss of glutamatergic synaptic contacts of cortico-neostriatal projections, similar to the neostriatal downregulation of glial glutamate transporters GLT1 and GLAST described by Levy et al (36) after cortical glutamatergic deafferentation.

The absence of GFAP, which is thought to be the principal cytoskeletal protein in astrocytes (37), in the majority of astrocytes with GLT1 transcripts, but its presence in nearly all GLT1mRNA containing astrocytes in neostriatum of HD, is a noteworthy side observation, indicating that in areas without astrogliosis, only a subpopulation of astrocytes expresses GFAP and that either only this subpopulation proliferates or that proliferating astrocytes start to express GFAP. According to O'Callaghan (38), enhanced GFAP occurring with reactive gliosis represents a potential biomarker of neurotoxicity. Although postmortem delay was similar and type and duration of fixation and enzymatic pretreatment was the same for control and HD tissue, false negative immunohistochemical results might occur due to the affinity of our monoclonal antibody to an epitope that is mainly accessible when glial filament bundles are dissociated and/or the soluble fraction of filaments is increased (37, 39).

The reduction of NR1, NR2B, and GLT1mRNA expression in neostriatum was heterogeneous. The loss of hybridization signals showed the same dorso-ventral progression in the putamen, corresponding to the progression of neuronal degeneration described by several authors (25, 34, 40). The characteristic gradient of neuronal loss in caudate reported by Vonsattel et al (25), with a relative preservation of the lateral part in comparison with the paraventricular portion of the caudate, correlated with the preservation of hybridization signals for NR1, NR2B and

GLT1mRNA in our case with the lowest neuropathological grade (grade 2). In the caudate of the other 2 cases (neuropathological grades 3 and 4), the signals were better preserved in the paraventricular in comparison with the lateral part. This might be due to individual differences in degeneration.

Furthermore, there were zones with pronounced hybridization signals for both NMDA receptor subunit and glutamate transporter transcripts corresponding to the remaining calbindin-D-rich matrix compartment. These areas consisted of a larger number of cells with enhanced mRNA levels compared with neighboring calbindin-D-poor areas representing striosomes and degenerated matrix. The characteristic loss of matrix in HD, as described by Seto-Ohshima et al (40), was parallel to a loss of hybridization signals for NR1, NR2B, and GLT1mRNA. Intriguingly, the loss of NR1/NR2B transcripts was nearly complete in the putamen at neuropathological grade 3 despite a preservation of the ventral matrix compartment; only a few neurons with low hybridization signals for NR1/NR2BmRNA were still detectable. These observations indicate a downregulation of NMDA receptor mRNA before neuronal degeneration. Since the neuronal degeneration proceeds, other neuronal populations, which do not express NMDA receptors, might also be involved in the process of degeneration. Hedreen and Folstein (34) found an early decrease of neostriatal striosome neurons. Since cases of neuropathological grades 0 and 1 were not available for this study, we were not able to determine if striosome neurons expressing NMDA receptor subunit mRNA are involved in this early degeneration. But our observation that even in the relatively well-preserved ventral putamen in our case with the lowest neuropathological grade, both number and mRNA levels of neurons with NR1/NR2B transcripts were lower in calbindin-D-poor areas than in calbindin-D-rich areas, makes it very likely that a degeneration of neurons expressing NMDA receptor subunit mRNA occurs first in striosomes and later in the matrix.

In contrast to putamen, NR1/NR2BmRNA expression was still detectable at neuropathological grade 4 in the caudate. This suggests the existence of NR1/NR2B mDNA expressing neurons with different vulnerabilities in the caudate and putamen.

Surprisingly, in our case with the lowest neuropathological grade, the cellular NR1 and NR2BmRNA expression was enhanced, particularly in zones with striking hybridization signals compared with corresponding neurons of controls. Since the pharmacological treatment of all 3 patients was similar in the last months before death, consisting of an irregular application of neuroleptics with weak antipsychotic effect such as sulpiride and promazine, it is unlikely that this "upregulation" is caused by medication. Thus, it is possible that an abnormal number of NMDA-receptor proteins resulted that could be involved in or even be responsible for an excitotoxic effect of glutamate (9). The parallel existence of neostriatal neurons with different NR1/NR2BmRNA levels in our case with the lowest neuropathological grade being higher, similar and lower than levels in controls, and the smaller number of neurons with NR1/NR2B transcripts having constantly lower mRNA levels at later stages suggest a gradual decrease of cellular NR1/NR2BmRNA expression before neuronal death.

CONCLUSION

According to our findings, a possible sequence of pathophysiological mechanisms of neurodegeneration in HD could be: (a) neuronal excitotoxic effect of glutamate due to an increased number of NMDA-receptors and/or due to abnormally sensitive NMDA-receptors; (b) astrogliosis representing an increased number of GLT1mRNA-expressing astrocytes as a compensatory mechanism to remove glutamate from the synaptic cleft; (c) degradation of cellular NR1/NR2BmRNA expression due to cell degeneration; (d) loss of neurons with NMDA receptors; (e) loss of synaptic glutamatergic contacts; (f) downregulation of glutamate transporter mRNA in astrocytes.

To further elucidate the pathogenesis of HD it will be necessary to investigate presymptomatic cases and cases of neuropathological grade 0 and 1.

According to the findings presented, neurons with NMDA receptors are impaired in the neostriatum of HD. The proliferation of astrocytes expressing membrane-bound glutamate transporters may represent a compensatory mechanism to protect neostriatal neurons from the excitotoxic effect of glutamate. This suggests that treatment with glutamate receptor antagonists in early phases of HD may be a useful approach.

ACKNOWLEDGMENTS

We thank Dr H. Lange, Neurological Therapy Centre, University of Düsseldorf, Prof. Dr B. Helpap, Department of Pathology, Singen, Prof. Dr Schröder, Department of Neuropathology, University of Cologne, and the Reference Center for Neurodegenerative Disease, University of Munich, for providing brain tissue specimens, Dr M. Gräber, Dr S. Kösel, and Prof. Dr P. Mehrain, Department of Neuropathology, Munich, for routine histopathological screening, Dr T. Meitinger, Department of Pediatric Genetics, University of Munich, for determination of CAG repeats. We especially thank Mrs S. Tauriainen-Ballin, Mrs R. Schneider, and Dr P. Sartorello for excellent technical assistance, Mr R. Erben for photographical assistance, and Mr H. Riescher for advice concerning computer programs. Part of this work was presented as a preliminary report in abstract form at the 2nd Congress of the European Society for Clinical Neuropharmacology, Würzburg, November 9–11, 1995 (J Neural Transm 1995;102:II).

REFERENCES

1. The Huntington's Disease Collaborative Research Group. A novel gene containing a trinucleotide repeat that is expanded and unstable on Huntington's disease chromosomes. Cell 1993;72:971–83

2. Albin RL, Tagle DA. Genetics and molecular biology of Huntington's disease. Trends Neurosci 1995;18:11–14
3. Martin JB, Gusella JF. Huntington's Disease—Pathogenesis and management. N Engl J Med 1986;315:1267–76
4. Forno LS, Jose C. Huntington's chorea: A pathological study. In: Barbeau A, Chase TN, Paulson GW, eds. Huntington's chorea. Advances in Neurology. Vol. I. New York: Raven Press, 1973:453–70
5. Kowall NW, Ferrante RJ, Martin JB. Patterns of cell loss in Huntington's disease. Trends Neurosci 1987;10:24–29
6. Reiner A, Albin RL, Anderson KD, D'Amato C, Penney JB, Young BY. Differential loss of striatal projection neurons in Huntington's disease. Proc Natl Acad Sci 1988;85:5733–37
7. Albin RL, Reiner A, Anderson KD, et al. Preferential loss of striato-external pallidal projection neurons in presymptomatic Huntington's disease. Am Neurol 1992;31:425–30
8. Richfield EK, Maguire-Zeiss KA, Vonkeman HE, Voorn P. Preferential loss of preproenkephalin versus preprotachykinin neurons from the striatum of Huntington's disease patients. Ann Neurol 1995;38:852–61
9. Bruyn GW. Huntington's chorea: Historical, clinical and laboratory synopsis. In: Vinken PJ, Bruyn GW, eds. Handbook of clinical neurology. Vol. 6. Amsterdam: North Holland, 1968:379–96
10. Divac I, Fonnum F, Storm-Mathisen. High affinity uptake of glutamate in terminals of corticostriatal axons. Nature 1977;266:377–88
11. Graybiel AM. Neurotransmitters and neuromodulators in the basal ganglia. Trends Neurosci 1990;13:244–54
12. Whetsell WO. Current concepts of excitotoxicity. J Neuropathol Exp Neurol 1996;55:1–13
13. Monyer H, Sprengel R, Schoepfer R, et al. Heteromeric NMDA receptors: Molecular and functional distinction of subtypes. Science 1992;256:1217–21
14. Foldes RL, Rampersad V, Kamboj RK. Cloning and sequence analysis of additional splice variants encoding human N-methyl-D-aspartate receptor (hNR1) subunits. Gene 1994;147:303–4
15. Foldes RL, Adams SL, Fantaske RP, Kamboj RK. Human N-methyl-D-aspartate receptor modulatory subunit hNR2A: Cloning and sequencing of the cDNA and primary structure of the protein. Bba Mol Cell Res 1994;1223:155–59
16. Adams SL, Foldes RL, Kamboj RK. Human N-methyl-D-aspartate receptor modulatory subunit hNR3: Cloning and sequencing of the cDNA and primary structure of the protein. Bba Gene Struct Express 1995;1260:105–8
17. Shashidharan P, Plaitakis A. Cloning and characterization of a glutamate transporter cDNA from human cerebellum. Biochim Biophys Acta 1993;1216:161–64
18. Shashidharan P, Wittenberg I, Plaitakis A. Molecular cloning of human brain glutamate/aspartate transporter II. Bba Biomembranes 1994;1191:393–96
19. Shashidharan P, Huntley GW, Meyer T, Morrison JH, Plaitakis A. Neuron-specific human glutamate transporter: Molecular cloning, characterization and expression in human brain. Brain Res 1994; 662:245–50
20. Rothstein JD, Martin L, Levey AI, et al. Localization of neuronal and glial glutamate transporters. Neuron 1994;13:713–25
21. Lehre KP, Levy LM, Ottersen OP, Storm-Mathisen J, Danbolt NC. Differential expression of two glial glutamate transporters in the rat brain: Quantitative and immunocytochemical observations. J Neurosci 1995;15:1835–53
22. Gerfen CR, Baimbridge KG, Miller JJ. The neostriastal mosaic: Compartmental distribution of calcium-binding protein and parvalbumin in the basal ganglia of the rat and monkey. Proc Natl Acad Sci USA 1985;82:8780–84
23. Bignami A, Eng LF, Dahl D, Uyeda CT. Localization of the glial fibrillary acidic protein in astrocytes by immunofluorescence. Brain Res 1972;43:429–35
24. Steinert PM. Intermediate filaments: Conformity and diversity of expression and structure. Ann Rev Cell Biol 1985;1:41–65
25. Vonsattel J-P, Myers R, Stevens TJ, Ferrante JR, Bird ED, Richardson EP. Neuropathological classification of Huntington's disease. J Neuropathol Exp Neurol 1985;44:559–77
26. Wisden W, Morris BJ, Hunt SP. In situ hybridization with synthetic DNA probes. In: Chad J, Wheal H, eds. Molecular neurobiology—a practical approach. Vol II. Oxford: IRL Press, 1991:205–25
27. Akbarian S, Sucher NJ, Bradley, D, et al. Selective alterations in gene expression for NMDA receptor subunits in prefrontal cortex of schizophrenics. J Neurosci 1996;16:19–30
28. Lange H, Thörner G, Hopf A, Schröder KF. Morphometric studies of the neuropathological changes in choreatic diseases. J Neurol Sci 1976;28:401–25
29. Dure IV LS, Young AB, Penney JB. Excitatory amino acid binding sites in the caudate nucleus and frontal cortex of Huntington's disease. Ann Neurol 1991;30:785–93
30. Young AB, Greenamyre JT, Hollingsworth Z, et al. NMDA receptor losses in putamen from patients with Huntington's disease. Science 1988;241:981–83
31. Williams K. Modulation of the N-methyl-D-aspartate receptor by polyamines: Molecular pharmacology and mechanisms of action. Biochem Soc Trans 1994;22:884–87
32. Illarioshkin SN, Igarashi S, Onodera O, et al. Trinucleotide repeat length and rate of progression of Huntington's disease. Ann Neurol 1994;36:630–34
33. Furtado S, Suchowersky O, Rewcastle B, et al. Relationship between trinucleotide repeats and neuropathological changes. Ann Neurol 1996;39:132–36
34. Hedreen JC, Folstein SE. Early loss of neostriatal striosome neurons in Huntington's disease. J Neuropath Exp Neurol 1995;54:105–20
35. Cross AJ, Slater P, Reynolds GP. Reduced high-affinity glutamate uptake sites in the brains of patients with Huntington's disease. Neurosci Lett 1986;67:198–202
36. Levy LM, Lehre KP, Walaas SI, Storm-Mathisen J, Danbolt NC. Down-regulation of glial glutamate transporters after glutamatergic denervation in the rat brain. Eur J Neurosci 1995;7:2036–41
37. Eng LF, Ghirnikar RS. GFAP and astrogliosis. Brain Pathol 1994;4: 229–37
38. O'Callaghan JP. Assessment of neurotoxicity: Use of glial fibrillary acidic protein as a biomarker. Biomed Environment Sci 1991;4: 197–206
39. McLendon RE, Bigner DD. Immunohistochemistry of the glial fibrillary acidic protein: Basic and applied considerations. Brain Pathol 1994;4:221–28
40. Seto-Ohshima A, Emson PC, Lawson E, Mountjoy CQ, Carrasco LH. Loss of matrix calcium-binding protein-containing neurons in Huntington's disease. Lancet 1988;i:1252–55

Received August 1, 1996
Revision received December 11, 1996
Accepted December 12, 1996